# NE8 Assignment 2: Discrete Ordinates

Andy Zhang

February 2025

The code for exercises 1-6 can be found in `aqz22_Zhang_A_NE8_Assignment2_Code_Ex1-6.py`. The code for exercise 7 is found in `aqz22_Zhang_A_NE8_Assignment2_Code_Ex7.py`. All of the code has been fully annotated.

Unless otherwise stated, all computations are done with a mesh resolution of 10 points/cm and $\phi$ normalized such that the total areal power $P = 1$ kW/cm$^2$. The convergence criteria is: $\max |\phi^{(j+1)} - \phi^{(j)}|/\phi^{(j)} < 0.00001$. The same material properties are used as were given in `Assignment 1: Diffusion`. Fission products such as $^{135}_{54}$Xe and $^{149}_{62}$Sm are ignored. Relevant macroscopic constants (before the transport correction) are:

$$\begin{aligned} \Sigma_\mathrm{s} &= 0.695409 \text{ cm}^{-1} \\ \nu\Sigma_\mathrm{f} &= 0.097624 \text{ cm}^{-1} \\ \Sigma_\mathrm{a} &= 0.067476 \text{ cm}^{-1} \\ \Sigma_\mathrm{t} &= 0.762886 \text{ cm}^{-1} \\ D &= 0.521483 \text{ cm} \end{aligned} \tag{1}$$

The analytical solution is known:

$$\begin{aligned} k_\mathrm{eff} &= 1.4362992876133593 \\ \phi &= 12287064062530.033 \cos(x/32.5385185) \text{ cm}^{-2}\text{s}^{-1} \end{aligned} \tag{2}$$

where $x$ is the position in cm. Note that this solution is also normalized such that $P = 1$ kW/cm$^2$ for a 100 cm slab. For the derivation of Equation 2, refer to Appendix A.

## 1 Discrete Ordinates Solver

### *1.1 "Write a discrete ordinates/SN solver for 1D slab geometry problems using the Gauss-Legendre quadrature, diamond-difference closure, and a 0.00001 convergence criterion on the flux."*

A 1D discrete ordinates solver using the Gauss-Legendre quadrature and diamond-difference closure was written according to the method outlined in Section 3 of the `NE8 Lecture 4: the discrete ordinates/SN method` document. One peculiarity is that the document only specifies how compute the source vector $Q^{(j+1)}$ from $\phi^{(j)}$ if the vectors are continuous. However, the computations are done on a mesh, where $\phi_i^{(j+1)}$ is computed from the value of $Q^{(j+1)}$ at the positions between the mesh points: $Q_{i+1/2}^{(j+1)}$. This problem was solved by assuming that $Q$ changes linearly over the intervals between the mesh points:

$$Q_{i+1/2} = (Q_i + Q_{i+1})/2 \tag{3}$$

As for the multiplication by $\nu\Sigma_f$, the same discretization method as the one in `NE8 Assignment 1: Diffusion` was used. This method is discussed in the `NE8 Workshop 1 Finite Elements_Handout (1)` document.

### *1.2 "Report k and show the flux distribution for S2, S6, and S12 on a problem with identical geometry and cross sections to that in coursework 1. "*

A Gauss-Legendre quadrature of order $N$ is denoted $S_N$. The convergence and final distribution of $\phi$ for $S_2$, $S_6$, $S_{12}$ and the diffusion approach are shown in Figure 1. The resultant eigenvalues are shown in Table 1. A comparison of the $k_\mathrm{eff}$ convergence for $S_{12}$ and diffusion is shown in Figure 2.

### *1.3 "Comment on how this compares with neutron diffusion in terms of accuracy, number of iterations and runtime."*

Runtime, number of iterations and accuracy figures are shown in Table 1. The accuracy was determined by comparing the results with the analytical solution in Equation 2.

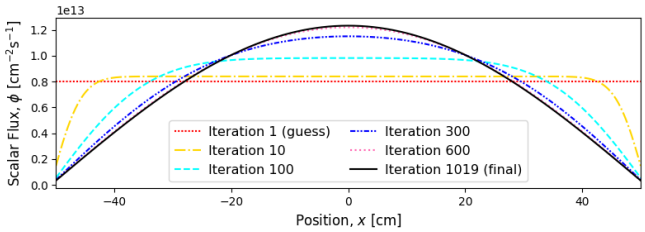


(a) Convergence of the discrete ordinates method with 2nd-order Gauss-Legendre quadrature set ($S_2$), and the diamond-difference closure relation.

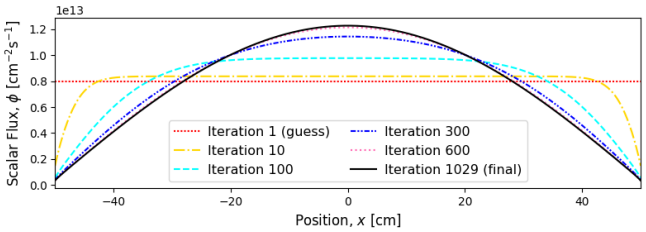


(b) Convergence of the discrete ordinates method with 6th-order Gauss-Legendre quadrature set ($S_6$), and the diamond-difference closure relation.

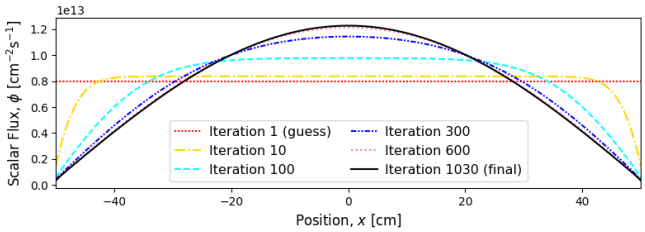


(c) Convergence of the discrete ordinates method with 12th-order Gauss-Legendre quadrature set ($S_{12}$), and the diamond-difference closure relation.

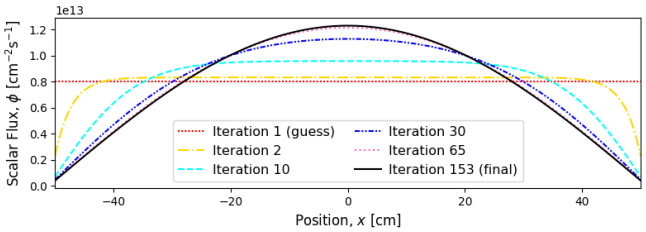


(d) Convergence of the neutron diffusion method, using the finite element approach and source iteration method.

Figure 1: Graphs depicting the convergence of the scalar neutron flux $\phi$ on a 100 cm slab using different computational methods.

Looking at Table 1, it is clear that the discrete ordinates method is a lot slower than the diffusion method, with the runtime increasing linearly with the order. The discrete ordinates method also requires many more iterations, but the exact number of iterations does not increase linearly with the order. As for the accuracy, the discrete ordinates method is more accurate when the order is high. However, lower orders such as $S_2$ results in a worse $k_{\text{eff}}$ than the diffusion method. The maximum relative error in $\phi$ is always worse for the discrete ordinates method.

### *1.4 "How does this compare with your expectations? What might explain your observations?"*

All of these observations are expected and can be explained.

The discrete ordinates method converges more slowly since it is directly trying to solve the transport equation. This means that the absorption and scattering are modeled directly, so these effects have to find equilibrium with each other before the process can converge. This is in contrast to the diffusion method, which approximates the combined effect of scattering and absorption together using the diffusion constant $D$. Since $D$ models the limiting behavior, the diffusion solver converges quickly. This quicker convergence can clearly be seen in Figure 2, as well as by comparing Figure 1d to the other graphs in Figure 1.

As for the runtime, the majority of the discrete ordinates method is taken up by the $\psi$ sweeps. These sweeps have to individually calculate values for all of the mesh points, so it is clearly the slowest process. The amount of times $\psi$ is calculated scales linearly with the order of the quadrature $N$. Therefore, the algorithmic complexity of the program is $O(N)$. This explains the scaling of the runtime in Table 1.

Regarding accuracy, the previous assignment showed that the diffusion approximation is valid for this setup. The advantage of the discrete ordinates method is that it considers the angular neutron fluxes when the quadrature order is high. This is why the discrete ordinates method only results in a more accurate $k_{\text{eff}}$ at higher orders.

The maximum relative error in $\phi$ is a misleading figure. This error occurs at the sides of the slab when $|x| = 50$ cm. At this position, the expected value of $\phi(50)$ is just 3.15% compared to the highest value. Therefore a small absolute error in $\phi$ can lead to a large relative error. All this number says is that the diffusion method is slightly more accurate at the very edges of the slab. Perhaps the maximum absolute error is a more insightful quantity.

Table 1: Comparison between the discrete ordinates method and the diffusion method. The columns are: the method used, the number of iterations before convergence, the resulting $k_{\text{eff}}$ and error compared to analytical, runtime, and maximum error in $\phi$ compared to analytical. All maximum $\phi$ errors are located at $|x| = 50$ cm.

| **Method** | **It.** | $k_{\text{eff}}$ | $k_{\text{eff}}$ **err.** | **Time** | **Max** $\phi$ **err.** |
|---|---|---|---|---|---|
| $S_2$ | 1019 | 1.4361960 | $7.19{\cdot}10^{-5}$ | 9.90 s | 17.961% |
| $S_6$ | 1029 | 1.4362832 | $1.12{\cdot}10^{-5}$ | 28.8 s | 18.616% |
| $S_{12}$ | 1030 | 1.4362865 | $8.91{\cdot}10^{-6}$ | 55.2 s | 18.642% |
| Diffusion | 153 | 1.4362695 | $2.98{\cdot}10^{-5}$ | 0.10 s | 5.924% |

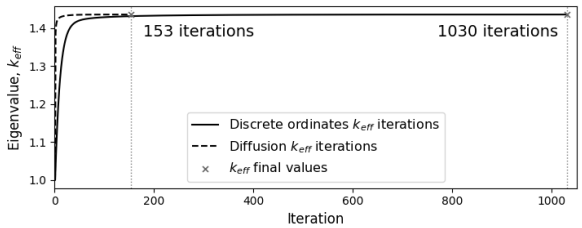


Figure 2: Graph depicting the convergence of $k_{\text{eff}}$ of the $S_{12}$ discrete ordinates method and the diffusion method.

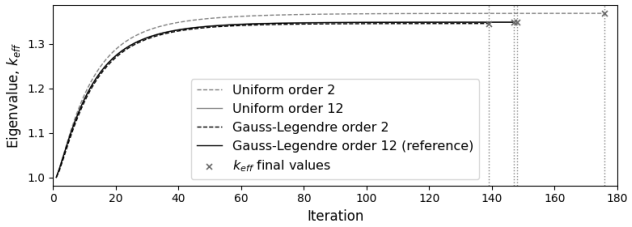


Figure 3: Graph depicting the convergence of $k_{\text{eff}}$ using different quadrature sets. Starting form the left, the vertical lines denote the iterations for $S_2$, $S_{12}$, $U_{12}$, and $U_2$ respectively.

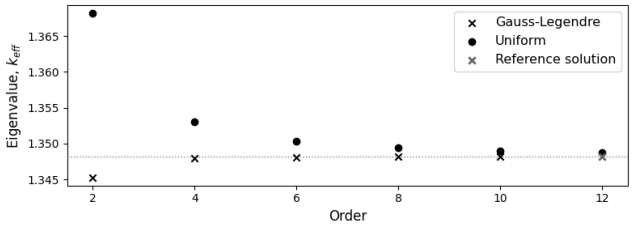


Figure 4: Graph depicting the results for $k_{\text{eff}}$ determined using different quadrature sets. The 12th-order Gauss-Legendre quadrature is taken as the reference solution.

# 2 Quadrature Study

*2.1 " Set the problem length to 30 cm. Generate an S12 solution using the Gauss-Legendre quadrature and take this as the reference solution. Replicate the quadrature study shown in Section 1.1 of the Discrete Ordinates: study the differences in the estimation of k between various orders of the Gauss-Legendre quadrature and a quadrature with equal spacing."*

Henceforth, the 'naive' equally spaced quadrature will be referred to as the *uniform* quadrature, denoted $U_N$. The different convergences of $k_{\text{eff}}$ is shown in Figure 3. The results for $k_{\text{eff}}$ are shown in Figure 4.

*2.2 "Comment on the results."*

Looking at Figure 3, $S_N$ quadratures tend to converge more quickly than their $U_N$ counterparts, while the difference shrinks for higher $N$. In addition, Figure 4 shows that $S_N$ quadratures are more accurate at equal $N$. This is important considering the previously mentionned algorithmic complexity of $O(N)$, so $N$ should ideally be as low as possible. It does appear that both quadratures asymptotically approach the same value. This makes sense as they are solving the same equation. It can be concluded that the Gauss-Legendre quadrature is superior in terms of both accuracy and speed of convergence.

# 3 Slab Length

*3.1 "Using S12 and your diffusion solver, vary the length of the problem from 5 cm to 5 m. Compare differences in k, the maximum relative difference in the flux, and show the number of iterations required."*

The problem size was varied over 25 different values between 5 cm and 5 m. The resolution was chosen such that there were always 101 mesh points. The maximum relative difference in $\phi$ is shown in Figure 5d, while several of the different $\phi$ distributions are shown in Figure 5a, Figure 5b, and Figure 5c. The differences in $k_{\text{eff}}$ are shown in Figure 5e and Figure 5f. The number of iterations for both methods are shown in Figure 5g, while the ratio between the 2 is shown in Figure 5h.

*3.2 "Comment on the results."*

The maximum relative difference in flux tends to decrease for longer slabs as shown in Figure 5d. This fact might be surprising, as naive comparison between Figure 5b and Figure 5c shows that the fluxes line up better at a slab length of 100 cm compared to 500 cm. However, this neglects the fact that the maximum relative difference in flux tends to happen at the edges of the slab, where the absolute value of $\phi$ is lowest. A closer look at the 2 figures reveals that the 500 cm slab has a slightly better alignment at the edges, leading to a lower relative flux error.

Comparing Figure 5a, Figure 5b, and Figure 5c, it appears that the diffusion approximation tends to be more spread out for shorter slabs, while becoming more narrow for longer slabs. The critical value at which the curves line up is around 100 cm. This length of 100 cm has interesting effects on the results below.

Figure 5e shows a large difference in $k_{\text{eff}}$ for short slabs, which rapidly becomes diminishes as the slab length is increased. From Figure 5f, it appears that the error first decreases exponentially before settling at some constant value after 150 cm. The kink between 100-150 cm is a sign change. Note 100 cm is when the diffusion solution starts becoming more narrow than the discrete ordinates one.

Comparing the iterations in Figure 5g shows that the discrete ordinates method requires many more iterations than the diffusion method. Figure 5h shows that the ratio between the two increases until 100 cm, before decreasing linearly. Again note the importance of the 100 cm slab.

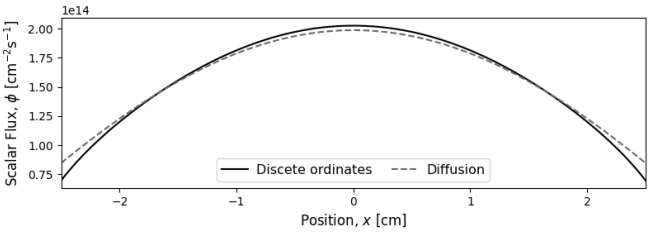


(a) Resultant flux distributions of a 5 cm slab calculated using the 2 methods.

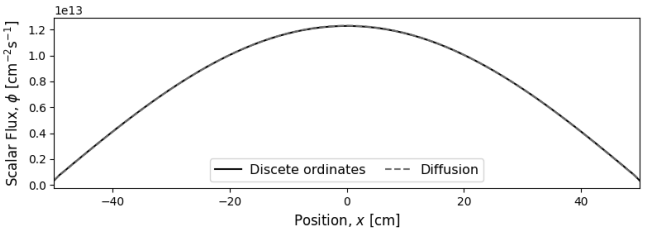


(b) Resultant flux distributions of a 100 cm slab calculated using the 2 methods.

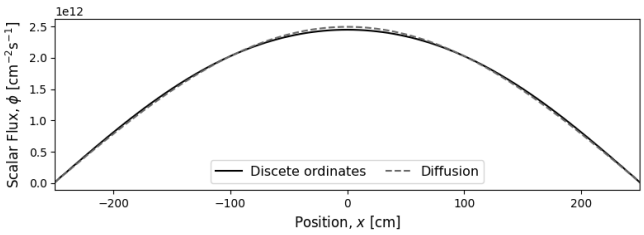


(c) Resultant flux distributions of a 500 cm slab calculated using the 2 methods.

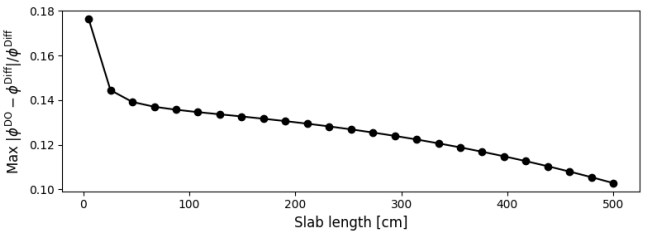


(d) Maximum relative difference in $\phi$ between the 2 methods for different slab lengths.

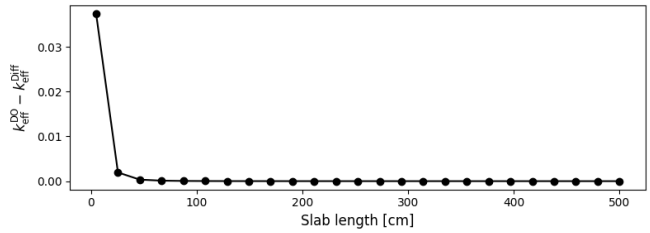


(e) Difference in $k_{\text{eff}}$ between the 2 methods for different slab lengths.

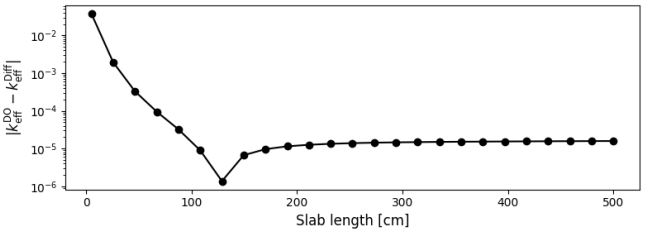


(f) Log-linear plot of the absolute difference in $k_{\text{eff}}$ between the 2 methods for different slab lengths.

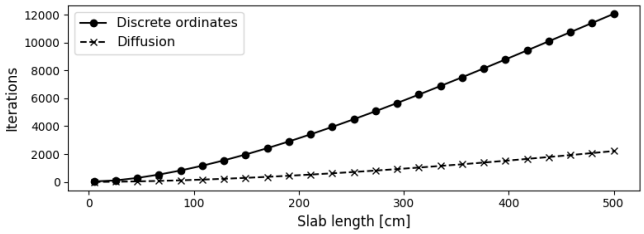


(g) Number of iterations required for the 2 methods at different slab lengths.

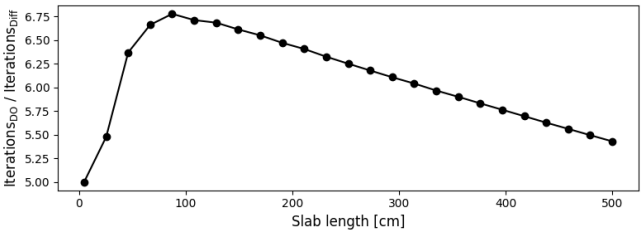


(h) Ratio of iterations required between the 2 methods at different slab lengths.

Figure 5: Graphs depicting several comparisons of discrete-ordinates and diffusion based solutions for slab lengths from 5 cm to 5 m.

# 4 Angular Fluxes

*4.1 "Fix the problem length at 100 cm and the quadrature at S12. On the final iteration of your simulation, store and report the angular fluxes in all direction in the centre of your problem and close to one of the edges."*

The angular fluxes are stored by saving the values of $\psi_n$ at the final iteration. However, $\psi$ only considers the angular fluxes in so far as they are projected onto the $x$-axis. This means that information regarding the orientation of $\psi$ in the $y, z$-plane is lost. For reasons of symmetry, it was assumed that $\psi$ stays constant around the $x$-axis.

*4.2 "Plot these in polar co-ordinates and comment on the results."*

Slices of the angular neutron flux at the left, center, and right of the slab are shown in Figure 6. Unsurprisingly, the angular distributions of $\psi$ in Figure 6a and Figure 6c point towards the outside of the slab. There are no neutrons entering the slab so all of the flux here is neutrons leaking out. As for the middle in Figure 6b, $\psi$ appears to be isotropic. This is unsurprising since the setup is symmetrical around $x = 0$ (note that the 1D transport equation ignores the $y$ and $z$ directions). As for the magnitude, $\psi$ is much larger in the center compared to the edges. This aligns with the flux distribution shown in Figure 1c.

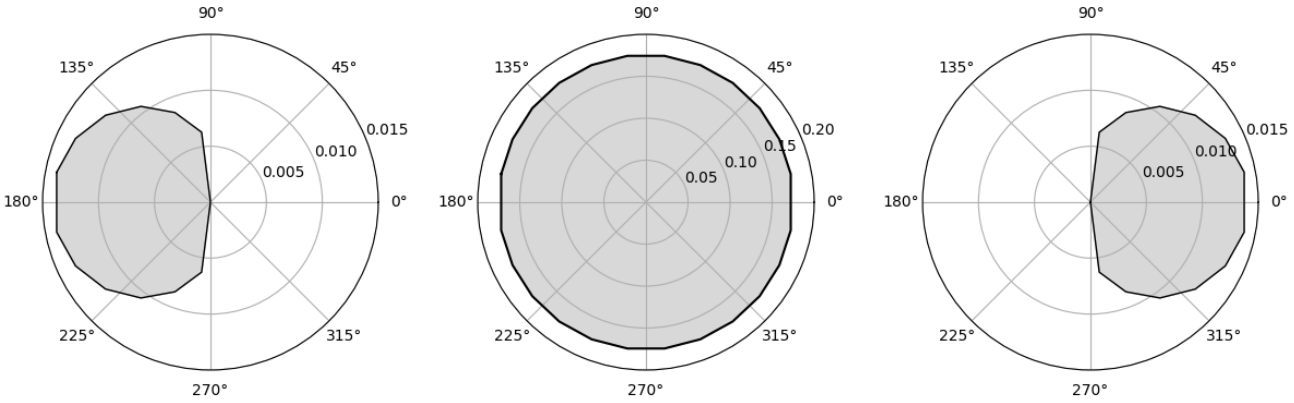


(a) Left side of the slab. (b) Middle of the slab. (c) Right side of the slab.

Figure 6: Polar plots of a slice of the the angular neutron flux $\psi$ at different positions in the slab. The horizontal angles of $0^\circ$ and $180^\circ$ corresponds to the $x$-axis of the slab. The units are in $\mathrm{cm}^{-2}\mathrm{s}^{-1}\mathrm{rad}^{-1}$.

# 5 Mesh Size

*5.1 "Fix the problem length at 100 cm and the quadrature at S12. Generate a reference solution and then vary the mesh size using both the diamond-difference closure and the step closure. Examine and comment on the maximum relative flux error versus mesh size."*

The reference solution was generated using Equation 2.

The maximum relative $\phi$ errors are shown in Figure 7. Looking at Figure 7a, the diamond-difference closure is much more accurate than the step closure at lower resolutions. This is especially apparent when looking at Figure 8, which depicts the flux distributions at low resolutions. Figure 8b clearly differs from the analytic solution at low resolutions. Interestingly, the step closure becomes more accurate than the diamond-difference method at certain higher resolutions, as shown in Figure 7b.

The error for both closure methods seems to converge towards some value around 18%. At a resolution of 100 points/cm, the diamond-difference closure has a maximum relative flux error of 18.64%, while the step closure has a maximum relative flux error of of 18.26%.

It should be noted the maximum relative flux error tends to happen at $|x| = 50$ cm, where the absolute value of $\phi$ is the smallest. In this location, a small absolute difference in flux can lead to a large relative flux error.

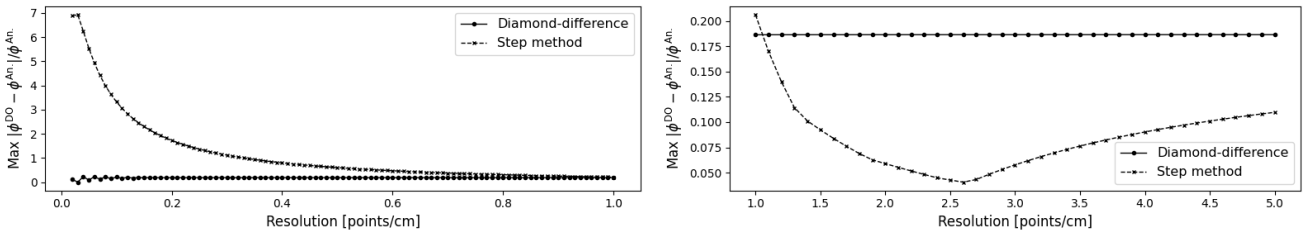


(a) Maximum relative flux error at resolutions in the range of $[0.02, 1]$ points/cm.

(b) Maximum relative flux error at resolutions in the range of $\langle 1, 5]$ points/cm.

Figure 7: Graphs showing the maximum relative error in the neutron flux $\phi$ using the discrete ordinates method with diamond-difference and step closures at different resolutions. The error is calculated in comparison to the analytical solution $\phi^{\mathrm{An.}}$.

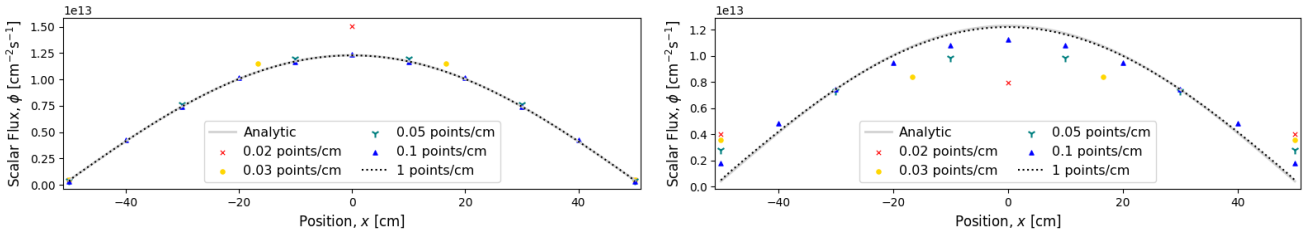


(a) Neutron flux using diamond-difference closure.

(b) Neutron flux using step closure.

Figure 8: Graphs depicting the converged neutron flux $\phi$ at different resolutions using different closures of the discrete ordinates method. The solid gray curves are the analytic solutions.

# 6 Scattering Ratio

*6.1 "Fix the problem length at 100 cm and the quadrature at S12. Modify the solver such that there is a source of neutrons at the left boundary which is isotropic across the half-sphere of directions pointing to the right. The boundary remains vacuum otherwise. Define c = Sigma s/Sigma tr as the scattering ratio. Make the slab non-multiplying but keep the value of Sigma tr fixed as before."*

The neutron source at the left boundary was implemented by setting the value of all the rightward pointing $\psi_{\mu>0}$ values to $\psi_{\mu>0}(x = -50) = 0.5$ cm$^{-2}$s$^{-1}$. This means that the source has a total strength of 0.5 cm$^{-2}$s$^{-1}$.

*6.2 "Produce a series of flux plots while varying the value of c over a wide range."*

The plots for a wide range of different values for $c$ are shown in Figure 9a, Figure 9b, Figure 9c, Figure 9d, and Figure 9e. Note that values of $c$ outside of $[0, 1]$ are nonsensical. The distribution for $c = 0$ was not plotted as it is uninteresting: 0.5 cm$^{-2}$s$^{-1}$, on the left and 0 everywhere else.

*6.3 "Comment on the number of iterations required and physical behavior of the system as c is varied."*

The number of iterations is shown in Figure 9f. The iterations appears to increase exponentially with higher values of $c$, peaking at 11963 iterations for $c = 1$. This is because the essence of the computation relies on the interaction between the neutron absorption $\Sigma_a$ (as a component of $\Sigma_{tr}$.) and the production from the previous generation, in this case: $\Sigma_s$. These are contradictory effects, so the algorithm is trying to find the equilibrium between these 2 counteracting forces. Since $\Sigma_s$ is directly applied to the previous generation, the algorithm relies on the $\Sigma_a$ to converge. An analogy would be that $\Sigma_a$ is trying to *push down* the erroneous peaks in $\psi$. Therefore, if $\Sigma_a$ is low compared to $\Sigma_s$, the problem converges more slowly. In this problem $c = \Sigma_s/(\Sigma_s + \Sigma_a)$, so a higher $c$ means a lower $\Sigma_a$ and a slower convergence. In general, higher values of $c$ means that more neutrons make it to the other side of the slab. This makes sense as less neutrons are being being absorbed. The trivial case of $c = 0$, simply corresponds to all neutrons being absorbed instantly.

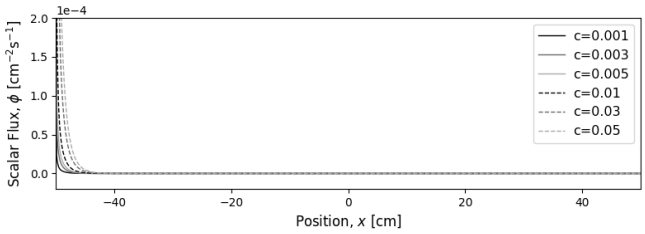


(a) Resultant flux distributions for several values of $c$ ranging from 0.001 to 0.05.

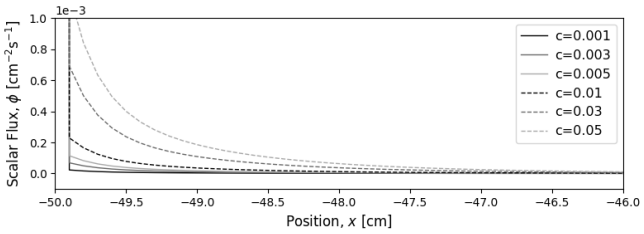


(b) Same flux distributions as in Figure 9a, but zoomed in to the $x = [-50, -46]$ range.

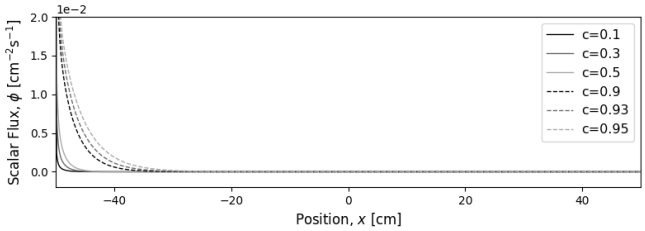


(c) Resultant flux distributions for several values of $c$ ranging from 0.1 to 0.95.

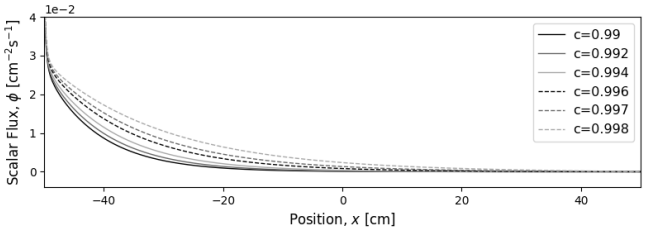


(d) Resultant flux distributions for several values of $c$ ranging from 0.99 to 0.998.

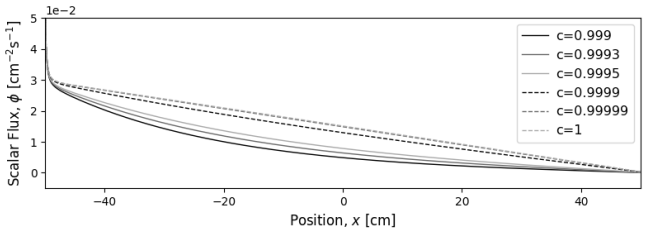


(e) Resultant flux distributions for several values of $c$ ranging from 0.999 to 1

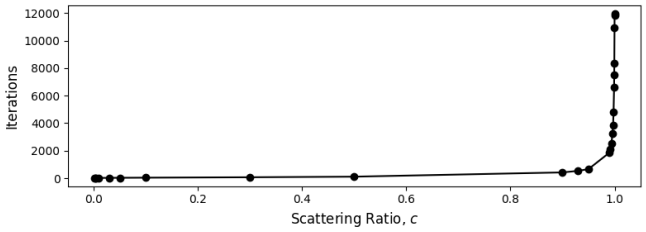


(f) Graph depicting the number of iterations before convergence for different values of $c$. $c = 1$ corresponds to 11963 iterations.

Figure 9: Graphs depicting several scattering ratio $c$ studies varied from $c = 0.001$ to $c = 1$. The setup is a non-multiplying slab of length 100 cm, with a 0.5 cm$^{-2}$s$^{-1}$ neutron source on the left side.

*6.4 "Also report and comment on any strange numerical behaviour observed."*

As expected, values of $c$ outside of $[0, 1]$ do not converge. They are nonphysical.

# 7 Two-Group Transport Simulation

For this exercise, please note that Dr Cosgrove had informed one of the students that the transport correction does not need to be considered. It will be assumed that the transport correction is already applied to the cross-sections provided.

*7.1 "Perform a two-group transport simulation for the geometry originally given in Q1. Neutrons are born fast and can be absorbed, scatter and remain in the same group, or scatter down to the thermal group. In the thermal group, neutrons can be absorbed, up-scatter, or scatter while remaining in the same group. Explain how you implement the two-group solver."*

Most of the transport algorithm is identical to the one described in subsection 1.1, as well as the `NE8 Lecture 4: the discrete ordinates/SN method` document. The difference is that there the algorithm is now applied to 2 different flux distributions: $\phi_1$, $\phi_2$, corresponding to the last and slow energies respectively. The calculation of the source vectors $Q_1, Q_2$ has to be changed to account for the interaction between the energy groups:

$$\begin{aligned} Q_1 &= [\ (\Sigma_{\mathrm{s},1\to1} + \chi_1\nu_1\Sigma_{\mathrm{f},1}/k_{\mathrm{eff}})\phi_1 \quad + \quad (\Sigma_{\mathrm{s},2\to1} + \chi_1\nu_2\Sigma_{\mathrm{f},2}/k_{\mathrm{eff}})\phi_2\ ]/2 \\ Q_2 &= [\ (\Sigma_{\mathrm{s},1\to2} + \chi_2\nu_1\Sigma_{\mathrm{f},1}/k_{\mathrm{eff}})\phi_1 \quad + \quad (\Sigma_{\mathrm{s},2\to2} + \chi_2\nu_2\Sigma_{\mathrm{f},2}/k_{\mathrm{eff}})\phi_2\ ]/2 \end{aligned} \tag{4}$$

The calculation of $k_{\mathrm{eff}}$ also has to take both energy groups into account:

$$k^{(j+1)} = k^{(j)} \frac{\sum_{i=1}^{I} \Delta x_i \left(\bar{\nu_1}\Sigma_{1,f,i}\,\phi_{1,i}^{(j+1)} + \bar{\nu_2}\Sigma_{f,2,i}\,\phi_{2,i}^{(j+1)}\right)}{\sum_{i=1}^{I} \Delta x_i \left(\bar{\nu_1}\Sigma_{1,f,i}\,\phi_{1,i}^{(j)} + \bar{\nu_2}\Sigma_{f,2,i}\,\phi_{2,i}^{(j)}\right)} \tag{5}$$

The convergence criteria was changed such that both $\phi_1$ and $\phi_2$ have to converge:

$$\max \frac{|\phi_1^{(j+1)} - \phi_1^{(j)}|}{\phi_1^{(j)}} < 0.00001 \quad \wedge \quad \max \frac{|\phi_2^{(j+1)} - \phi_2^{(j)}|}{\phi_2^{(j)}} < 0.00001 \tag{6}$$

The two-group transport simulation was run using the $S_{12}$ quadrature and the diamond difference closure relation. The total areal power was normalized to $P = 1$ kW/cm$^2$.

*7.2 "Report the value of k and show the flux distributions in each energy group, explaining their similarities or differences."*

The resultant flux distributions are shown in Figure 11. Clearly, most of the neutron flux is in the fast group. The convergence of $\phi_1$ and $\phi_2$ are shown in Figure 12. Comparing Figure 12a and Figure 12b, both $\phi_1$ and $\phi_2$ appear to have a similar shape. This is not just true for the final converged solution, but also for the iterations. This makes sense as the relationship between the 2 groups is determined by scalar quantities that are constant in space.

Finally, the convergence of $k_{\mathrm{eff}}$ is shown in Figure 10. This value converges very quickly so only a portion of the convergence is shown. Interestingly, the value peaks in the first few iterations before quickly dropping to the final value. The peak might be explained by the fact that the ratio between $\phi_1$ and $\phi_2$ is inaccurate in the first few iterations. This can clearly be seen by comparing the iteration 1 and iteration 10 curves in Figure 12. The final value for $k_{\mathrm{eff}}$ was determined to be:

$$k_{\mathrm{eff}} = 1.240178760329047 \tag{7}$$

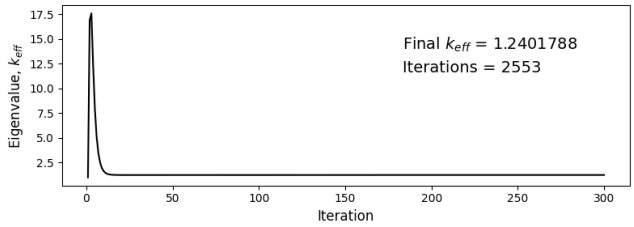


Figure 10: Graph depicting a portion of the eigenvalue $k_{\mathrm{eff}}$ convergence for the 2-group transport simulation.

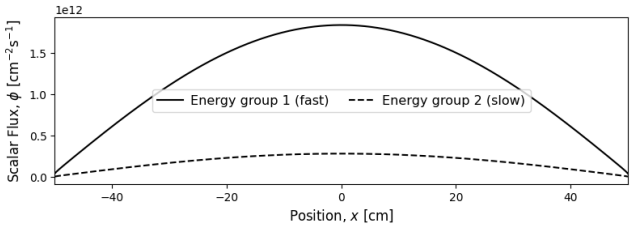


Figure 11: Graph depicting the scalar neutron fluxes $\phi_1$ and $\phi_2$ for the 2-group transport simulation.

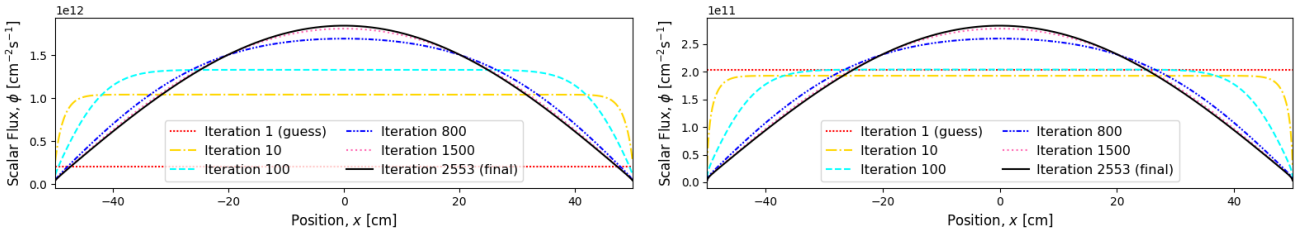


(a) Convergence of the fast neutron group $\phi_1$.

(b) Convergence of the slow neutron group $\phi_2$.

Figure 12: Graphs depicting the convergence of the scalar neutron flux $\phi$ for the 2 different energy groups using the discrete ordinates neutron transport method ($S_{12}$).

# A Derivation of the Analytical Solution

The following derivation was taken from my report for `NE8 Assignment 1: Diffusion`, exercise 4.

The diffusion equation with a fission source is given by:

$$-\frac{\mathrm{d}}{\mathrm{d}x}D\frac{\mathrm{d}}{\mathrm{d}x}\phi + \left(\Sigma_\mathrm{a} - \frac{\nu\Sigma_\mathrm{f}}{k_\mathrm{eff}}\right)\phi = 0 \tag{8}$$

where $k_\mathrm{eff}$ is the unknown eigenvalue that needs to be computed. Define $L$ as:

$$L = \sqrt{\frac{D}{\frac{\nu\Sigma_\mathrm{f}}{k_\mathrm{eff}} - \Sigma_\mathrm{a}}} \tag{9}$$

Substitute Equation 9 in Equation 8 and simplify.

$$\frac{\mathrm{d}^2\phi}{\mathrm{d}x^2} = -\frac{1}{L^2}\phi \tag{10}$$

Solve by inspection. Note that the setup is symmetric around $x = 0$, so the solution must be even.

$$\phi = A\cos(x/L) \tag{11}$$

By definition, $\phi$ vanishes at a distance of extrapolation distance $z_0$ outside the slab.

$$\cos\left(\pm\frac{50 + z_0}{L}\right) = 0 \tag{12}$$

Since $\phi \geqslant 0$, these must be the first roots of the cosine.

$$\frac{50 + z_0}{L} = \frac{\pi}{2} \tag{13}$$

Solve for $L$ and expand using Equation 9.

$$\sqrt{\frac{D}{\frac{\nu\Sigma_\mathrm{f}}{k_\mathrm{eff}} - \Sigma_\mathrm{a}}} = \frac{2(50 + z_0)}{\pi} \tag{14}$$

Solve for $k_\mathrm{eff}$.

$$k_\mathrm{eff} = \frac{\nu\Sigma_\mathrm{f}}{\frac{D}{4}\left(\frac{\pi}{50 + z_0}\right)^2 + \Sigma_\mathrm{a}} \tag{15}$$

The extrapolation distance was given in `NE8 assignment 1: Diffusion`, ex. 4.

$$\begin{aligned} z_0 &= 0.7104\lambda_\mathrm{tr} \\ &= 0.7104/\Sigma_\mathrm{tr} \end{aligned} \tag{16}$$

So the analytic solution becomes:

$$k_\mathrm{eff} = \frac{\nu\Sigma_\mathrm{f}}{\frac{D}{4}\left(\frac{\pi}{50 + 0.7104/\Sigma_\mathrm{tr}}\right)^2 + \Sigma_\mathrm{a}} \tag{17}$$

The resultant $k_\mathrm{eff}$ value is:

$$k_\mathrm{eff} = 1.4362992876133593 \tag{18}$$

The analytic solution for $\phi$ is then found using Equation 11, where $L$ is defined according to Equation 9 and $A$ was chosen such that the total areal power $P = 1$ kW/cm$^2$.

$$\phi \;=\; 12287064062530.033\cos(x/32.5385185)\ \mathrm{cm}^{-2}\mathrm{s}^{-1} \tag{19}$$